Journal of Alloys and Compounds 509 (2011) 7803–7807

Contents lists available at ScienceDirect

Journal of Alloys and Compounds

journal homepage: www.elsevier.com/locate/jallcom

Perpendicular magnetic anisotropy in 70 nm $CoFe_2O_4$ thin films fabricated on SiO_2/Si(1 0 0) by the sol–gel method

X.W. Wang, Y.Q. Zhang*, H. Meng, Z.J. Wang, Z.D. Zhang

Shenyang National Laboratory for Materials Science, Institute of Metal Research, and International Center for Materials Physics, Chinese Academy of Sciences, 72 Wenhua Road, Shenyang 110016, People's Republic of China

ARTICLE INFO

Article history:
Received 6 January 2011
Received in revised form 3 May 2011
Accepted 5 May 2011
Available online 12 May 2011

Keywords:
$CoFe_2O_4$
Thin films
Sol–gel method
Magnetic anisotropy

ABSTRACT

Cobalt ferrite $CoFe_2O_4$ films were fabricated on SiO_2/Si(1 0 0) by the sol–gel method. Films crystallized at/above 600 °C are stoichiometric as expected. With increase of the annealing temperature from 600 °C to 750 °C, the columnar grain size of $CoFe_2O_4$ film increases from 13 nm to 50 nm, resulting in surface roughness increasing from 0.46 nm to 2.55 nm. Magnetic hysteresis loops in both in-plane and out-of-plane directions, at different annealing temperatures, indicate that the films annealed at 750 °C exhibit obvious perpendicular magnetic anisotropy. Simultaneously, with the annealing temperature increasing from 600 °C to 750 °C, the out of plane coercivity increases from 1 kOe to 2.4 kOe and the corresponding saturation magnetization increases from 200 emu/cm^3 to 283 emu/cm^3. In addition, all crystallized films exhibit cluster-like structured magnetic domains.

1. Introduction

Cobalt ferrite ($CoFe_2O_4$, CFO) has attracted much attention for its numerous technological applications such as high-density recording media, microwave devices, spin filtering and multiferroics due to its strong magnetocrystalline anisotropy, larger permeability at high frequency and good insulating property, large magnetostriction, higher Curie temperature etc. [1–8]. The modification of magnetic and dielectric properties of CFO can be realized through substitution [9–11], fabrication of monodispersed purified hollow ferrite spheres [12] and growth of CFO films on different substrates using various techniques such as sputtering, molecular beam epitaxy, pulsed laser deposition and sol–gel method [3,4,13–27]. Considering practical applications in magnetic recording, the sol–gel method is an attractive alternative to other deposition methods due to its advantages such as lower annealing temperature, easier composition control, non-vacuum process and easier fabrication of large area thin films [21,23]. The sol–gel method can also provide good control over the formation of ferrite particles with small grain size that are favored in high-density recording media [21,23,25].

The tailoring of magnetic anisotropy in CFO films can be achieved by tuning the stress state of the CFO films using different substrates, inserting a buffer layer as well as varying film thickness [17–20,23,26]. For example, in-plane alignment of the easy axis is observed in thick (such as 400 nm) CFO films grown on MgO, due to the existence of shape anisotropy. As the thickness decreases to a certain value (such as 60 nm), tensile strain in the films generates a perpendicular anisotropy, which overcomes the shape anisotropy and prevails in the films [20]. Thermal stresses, which arise due to the differences between the thermal expansion coefficients of substrate and film, is also an important and common stress affecting the properties of the obtained films [28,29]. Sol–gel derived polycrystalline CFO films studied in previous papers are thicker than 100 nm, and the stress will relax partly or mostly, leading to magnetic isotropy or in-plane (IP) anisotropy [21,22]. In this paper, the CFO films with a thickness of 70 nm are fabricated by the sol–gel method with subsequent annealing at different temperatures. It is found that all crystallized films exhibit cluster-like structured magnetic domains. Moreover, the crystallized films annealed at 750 °C show obvious perpendicular magnetic anisotropy due to the tensile stress arising from the difference in the thermal expansion coefficients of the substrate and the films.

2. Experimental

Measured amounts of $Fe(NO_3)_3{\cdot}6H_2O$ and $Co(NO_3)_2{\cdot}9H_2O$ in the molar ratio of 2:1 were dissolved in 2-methoxyethanol ($CH_3OCH_2CH_2OH$) by ultrasonic vibration. All the reagents are purchased from Sinopharm Chemical Reagent Co., Ltd. The solution was adjusted to 0.3 mol/L. The solution was spin-coated on oxidized silicon substrates (SiO_2/Si (1 0 0)) at 1000 rpm (revolutions per minute) for 18 s and then 3000 rpm for 50 s. The wet films were dried at 120 °C for 2 min and then pyrolyzed at 400 °C for 5 min. The precursor films were then annealed at 500–750 °C for 30 min in air with no magnetic field application while annealing.

The crystalline structure of CFO films was examined using X-ray diffractometry (XRD, D/max-2000) with Cu Kα radiation at 40 kV and 100 mA. X-ray photoelectron

* Corresponding author. Tel.: +86 24 23971856; fax: +86 24 23971215.
E-mail address: yqzhang@imr.ac.cn (Y.Q. Zhang).

0925-8388/$ – see front matter © 2011 Elsevier B.V. All rights reserved.
doi:10.1016/j.jallcom.2011.05.021

spectroscopy (XPS) studies were performed using a monochromatic Al Kα radiation (ESCALAB250, thermo VG), the binding energies of samples were calibrated by taking the carbon 1s peak as reference (285.5 eV). The surface morphology and magnetic domains of the films were investigated by using atomic force microscopy and magnetic force microscopy (AFM/MFM, Digital instruments Nanoscope IV). Magnetic properties of the films were measured by a superconducting quantum interference device (SQUID, Quantum Design) with a maximum field of 70 kOe.

3. Results and discussion

Fig. 1 shows XRD patterns of CFO thin films after annealing at different temperatures for 30 min. It is seen that the annealed CFO films are amorphous at 500 °C, and then crystallize to the spinel phase with a random orientation at/above 600 °C. With an increase of annealing temperature, the intensity of the major peak (3 1 1) becomes higher, indicating better crystallization with the increase of annealing temperature.

The wide-scan XPS spectra of the binding energies range from 0 to 1300 eV show that the CFO film contains Fe, Co, and O with no other impurity elements being found except carbon, which is probably due to airborne contaminations. The high-resolution narrow-scan XPS spectra of Fe 2p, Co 2p, O 1s and C 1 s peaks of the CFO films are shown in Fig. 2. Peaks of Fe $2p_{3/2}$ and Co $2p_{3/2}$ for all the films are found at the binding energy of 710.86 eV and 780.10 eV, corresponding to a valence state of Fe^{3+} and Co^{2+}, respectively [30,31]. In addition, the peaks of O 1s and C 1s are broadened

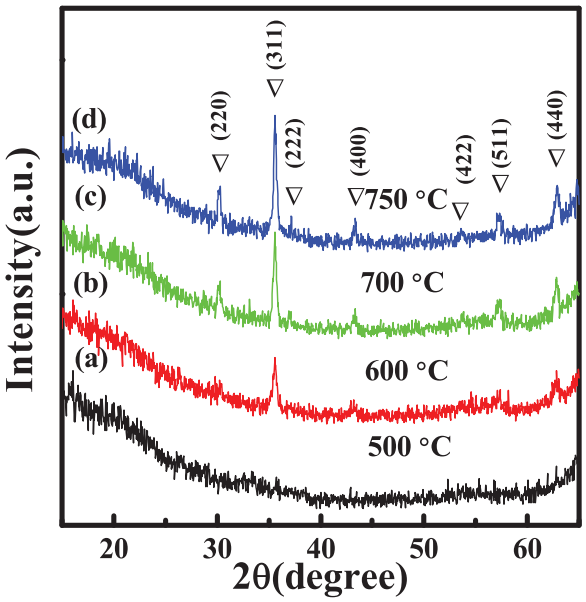

Fig. 1. XRD patterns of CFO films annealed (a) 500 °C, (b) 600 °C, (c) 700 °C and (d) 750 °C for 30 min.

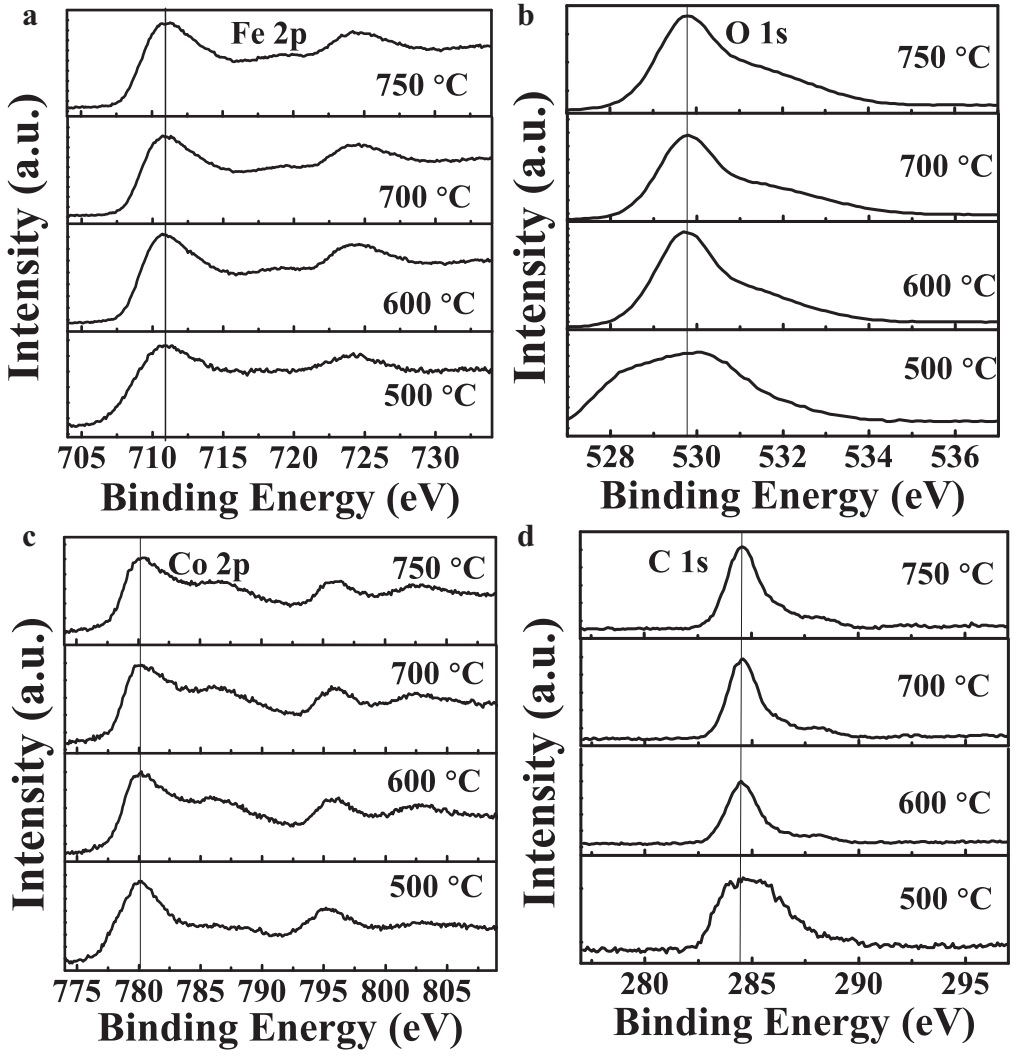

Fig. 2. XPS spectra of (a) Fe 2p, (b) Co 2p, (c) O 1s and (d) C 1s core levels for the CFO films annealed at 500–750 °C for 30 min.

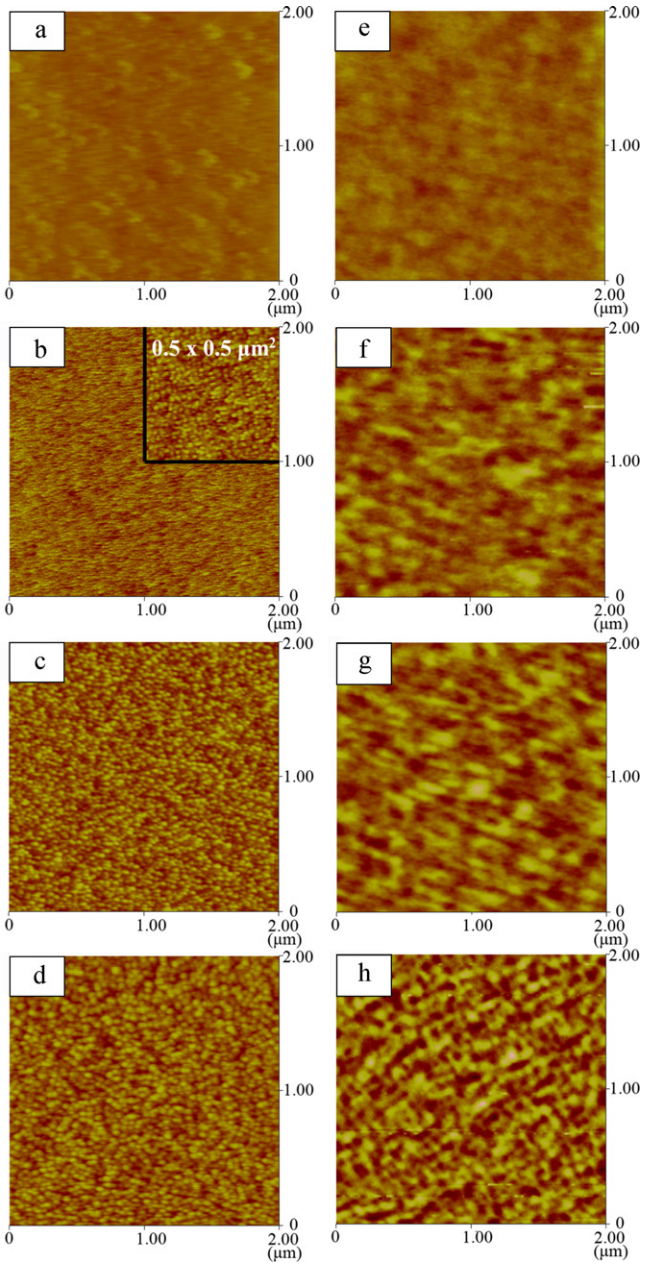

Fig. 3. AFM images ($2 \times 2\,\mu m^2$) (a)–(d) and MFM images (e)–(h) for CFO films annealed at 500 °C, 600 °C, 700 °C and 750 °C, respectively. Inset: AFM image in the area of $0.5 \times 0.5\,\mu m^2$ for CFO films annealed at 600 °C.

only for the CFO films annealed at 500 °C, indicating the existence of C and O mixtures. This may be attributed to the existence of some organic compounds. Through the analysis of the Co, Fe and O peaks, it is found that the Co:Fe:O ratio of the crystallized films is close to 1:2:4, indicating that the CFO films are stoichiometric, as expected.

Fig. 3(a)–(d) shows the surface morphology in $2 \times 2\,\mu m^2$ area for CFO films annealed at different temperatures, and the inset in Fig. 3(b) is the $0.5 \times 0.5\,\mu m^2$ surface morphology for CFO films annealed at 600 °C. For films annealed at 500 °C, the surface is very smooth with a root-mean-square (RMS) roughness of 0.20 nm. Some extraneous particles are observed on the surface which might be organic compounds or residual carbon due to the low annealing temperature. Small grains of about 13 nm are observed in the CFO films annealed at 600 °C, and with an increase of the annealing temperature up to 700 °C and 750 °C, the size of grains become

Table 1
The saturation magnetizations (Ms), remnant magnetizations (Mr) and coercive fields (Hc) in both directions for the CFO films annealed at different temperatures.

T (°C)	Ms (emu/cm^3)	Mr (emu/cm^3)		Hc (Oe)	
		IP	OOP	IP	OOP
500	150	23	18	300	300
600	185	58	52	1000	1000
700	265	95	98	1700	1600
750	283	91	102	2400	1600

30 nm and 50 nm, respectively. The RMS roughness of the films also increase with the annealing temperature, and are 0.46 nm, 1.47 nm and 2.55 nm for films annealed at 600 °C, 700 °C and 750 °C, respectively. Cross-sectional observations reveal that the crystallized films show columnar grain structure. Fig. 3(e)–(h) represents MFM images of the CFO films, corresponding to the surface morphologies in Fig. 3(a)–(d). The featureless graph is due to the amorphous structure of films annealed at 500 °C. For crystallized films, the MFM graphs consist of domains with a cluster-like structure where the magnetization is confined up and down with dark and clear contrast, respectively. The domain structure is similar to that observed in reference, but with a domain length of about 150 nm, which is much smaller than that in Ref. [32]. This might be attributed to the polycrystalline structure in our films.

Magnetic hysteresis loops of CFO films recorded in the in-plane (IP) and out-of-plane (OOP) directions at 295 K are shown in Fig. 4. The saturation magnetizations (Ms), remnant magnetizations (Mr) and coercive fields (Hc) in both directions are shown in Table 1. The films annealed at 500 °C show similar hysteresis loops in both directions with a coercive field of 300 Oe (1 Oe equals about 80 A/m) and saturation magnetization of 150 emu/cm^3. For the crystallized films annealed at 600–750 °C, the coercive field varies from 1 kOe to 2.4 kOe, which is comparable to the values in literature [21,22]. The increase of the coercive field with increasing annealing temperature could be attributed to the grain growth [33]. The saturation magnetization of CFO films have been found to increase with an increase of annealing temperature due to better crystallization and larger grain size [33–35], in particular, the saturation magnetization for the film annealed at 750 °C is 283 emu/cm^3, which is comparable with that in Refs. [13,21,26,33,34]. The remnant magnetization in the OOP direction is larger than that in the IP direction for the CFO films annealed at 750 °C. It is seen from all hysteresis loops that the crystallized CFO films annealed at 750 °C show obvious perpendicular magnetic anisotropy which could be attributed to the formation of columnar grains and thermal stress in the films [14,20]. On one hand, columnar grains create magnetic shape anisotropy with the easy axis being preferential to the column direction (OOP direction), however, the magnetic shape anisotropy of the column grain in the films is smaller than the magnetic shape anisotropy of the 2D film, whose demagnetization factor in the OOP direction is 1. Therefore, the columnar grain structure is not the main source of the perpendicular magnetic anisotropy in the CFO films. On the other hand, the larger difference in the thermal expansion coefficients of CFO (15 ppm/°C) and Si (4 ppm/°C) during the cooling process, together with a small thickness (70 nm), result in a larger tensile stress in the CFO films [26,36], and the tensile strain generates a perpendicular anisotropy due to a negative magnetostriction constant of the CFO film (about −200 ppm) [32]. The perpendicular anisotropy generated by tensile strain overcomes the magnetocrystalline anisotropy and the magnetic shape anisotropy of the 2D film, leading to the perpendicular anisotropy in the CFO polycrystalline films.

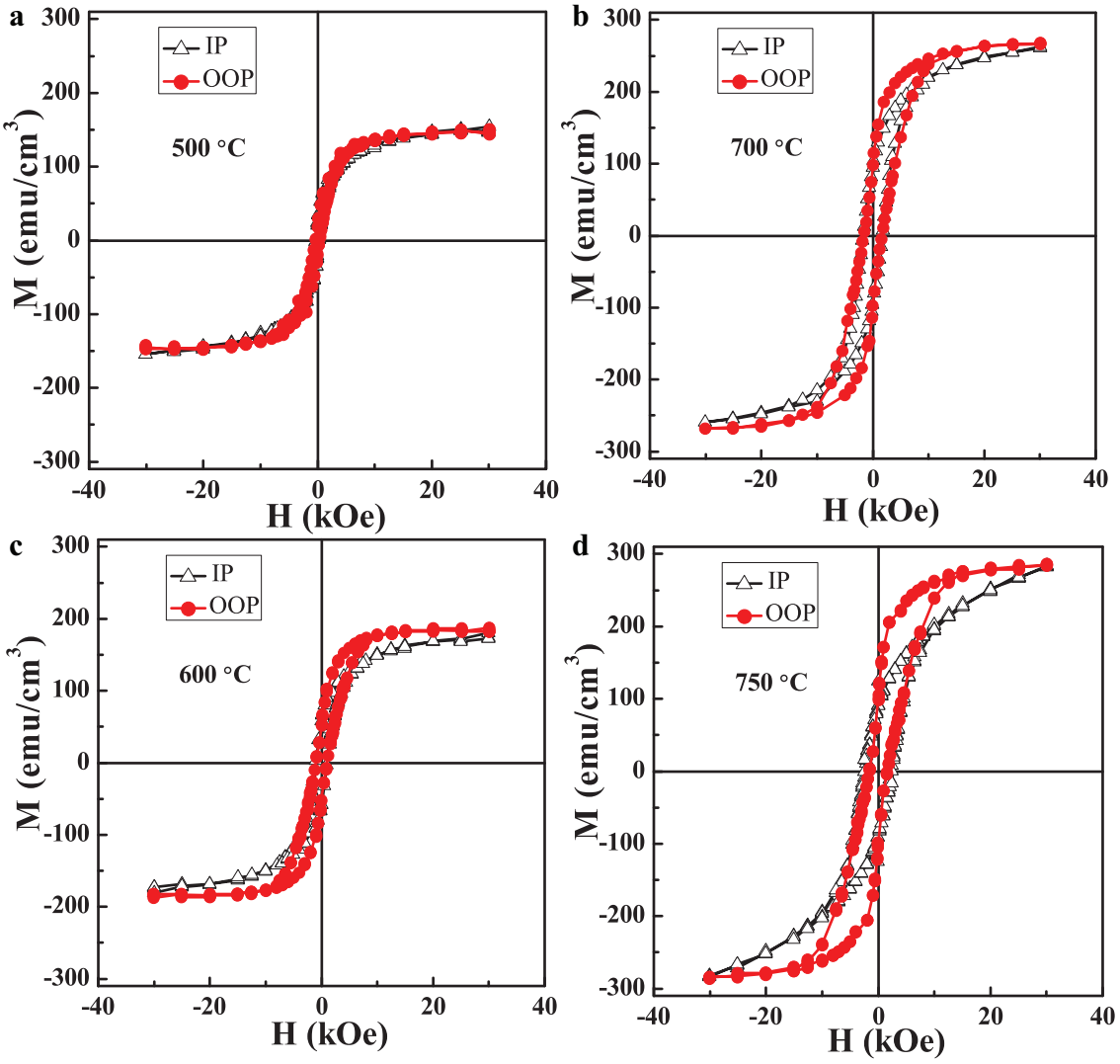

Fig. 4. Magnetic hysteresis loops in the in-plane (IP) and the out-of-plane (OOP) directions for the films annealed at (a) 500 °C, (b) 600 °C, (c) 700 °C and (d) 750 °C.

4. Conclusions

The microstructure and magnetic properties of 70 nm CFO thin films prepared by sol–gel method have been investigated. No spinel phase is detected in the CFO films annealed at 500 °C. CFO films annealed at/above 600 °C are stoichiometric with the spinel phase. The size of columnar grains and the RMS roughness of films increase with the annealing temperature increasing from 600 °C to 750 °C. Cluster-like magnetic domain structure is observed in all crystallized CFO films. The crystallized CFO films annealed at 750 °C show obvious perpendicular magnetic anisotropy, which could be mainly attributed to the thermal stress in the films.

Acknowledgments

This work has been supported by the Hundred Talents Program of Chinese Academy of Sciences, the National Natural Science Foundation of China (Nos. 50802098 and 51072202) and the National Basic Research Program No. 2010CB934603, the Ministry of Science and Technology of China.

References

[1] J. Ding, Y.J. Chen, Y. Shi, S. Wang, Appl. Phys. Lett. 77 (2000) 3621–3623.
[2] A. Goldman, Modern Ferrite Technology, Springer, New York, 2006.
[3] M. Gajek, M. Bibes, S. Fusil, K. Bouzehouane, J. Fontcuberta, A.E. Barthelemy, A. Fert, Nat. Mater. 6 (2007) 296–302.
[4] M.G. Chapline, S.X. Wang, Phys. Rev. B 74 (2006) 014418.
[5] M.S. Khandekar, R.C. Kambale, J.Y. Patil, Y.D. Kolekar, S.S. Suryavanshi, J. Alloys Compd. 509 (2011) 1861–1865.
[6] M. Sajjia, M. Oubaha, T. Prescott, A.G. Olabi, J. Alloys Compd. 506 (2010) 400–406.
[7] X.W. Tang, J.M. Dai, X.B. Zhu, W.H. Song, Y.P. Sun, J. Alloys Compd. 509 (2011) 4748–4753.
[8] A. Maqsood, K. Khan, J. Alloys Compd. 509 (2011) 3393–3397.
[9] S.S. More, R.H. Kadam, A.B. Kadam, A.R. Shite, D.R. Shite, D.R. Mane, K.M. Jadhav, J. Alloys Compd. 502 (2010) 477–479.
[10] R.C. Kambale, P.A. Shaikh, N.S. Harale, V.A. Bilur, Y.D. Kolekar, C.H. Bhosale, K.Y. Rajpure, J. Alloys Compd. 490 (2010) 568–571.
[11] I.H. Gul, A. Maqsood, J. Alloys Compd. 465 (2008) 227–231.
[12] W.C. Li, X.J. Qiao, Q.Y. Zheng, T.L. Zhang, J. Alloys Compd. 509 (2011) 6206–6211.
[13] J.H. Yin, J. Ding, B.H. Liu, X.S. Miao, J.S. Chen, J. Magn. Magn. Mater. 310 (2007) 2537–2539.
[14] M.C. Terzzoli, S. Duhalde, S. Jacobo, L. Steren, C. Moina, J. Alloys Compd. 369 (2004) 209–212.
[15] T.E. Quickel, V.H. Le, T. Brezesinski, S.H. Tolbert, Nano Lett. 10 (2010) 2982–2988.
[16] F. Rigato, J. Geshev, V. Skumryev, J. Fontcuberta, J. Appl. Phys. 106 (2009) 113924.
[17] W. Huang, J. Zhu, H.Z. Zeng, X.H. Wei, Y. Zhang, Y.R. Li, Appl. Phys. Lett. 89 (2006) 262506.
[18] A. Raghunathan, I.C. Nlebedim, D.C. Jiles, J.E. Snyder, J. Appl. Phys. 107 (2010) 09A516.
[19] T. Dhakal, D. Mukherjee, R. Hyde, P. Mukherjee, M.H. Phan, H. Srikanth, S. Witanachchi, J. Appl. Phys. 107 (2010) 053914.

[20] A. Lisfi, C.M. Williams, L.T. Nguyen, J.C. Lodder, A. Coleman, H. Corcoran, A. Johnson, P. Chang, A. Kumar, W. Morgan, Phys. Rev. B 76 (2007) 054405.
[21] J.G. Lee, J.Y. Park, Y.J. Oh, C.S. Kim, J. Appl. Phys. 84 (1998) 2801–2804.
[22] N.C. Pramanik, T. Fujii, M. Nakanishi, J. Takada, Mater. Lett. 59 (2005) 88–93.
[23] N.C. Pramanik, T. Fujii, M. Nakanishi, J. Takada, J. Mater. Sci. 40 (2005) 4169–4172.
[24] H. Ohashi, Y. Okazaki, Y. Ohya, S. Yanase, S. Hashi, IEEE Trans. Magn. 42 (2006) 2891–2893.
[25] E.S. Murdock, R.F. Simmons, R. Davidson, IEEE Trans. Magn. 28 (1992) 3078–3083.
[26] X.S. Gao, D.H. Bao, B. Birajdar, T. Habisreuther, R. Mattheis, M.A. Schubert, M. Alexe, D. Hesse, J. Phys. D: Appl. Phys. 42 (2009) 175006.
[27] G. Caruntu, A. Newell, D. Caruntu, C.J. O'Connor, J. Alloys Compd. 434–435 (2007) 637–640.
[28] O. Moshe, D.H. Rich, B. Damilano, J. Massies, Appl. Phys. Lett. 98 (2011) 061903.
[29] J. Zhang, M.W. Cole, S.P. Alpay, J. Appl. Phys. 108 (2010) 054103.
[30] Z.P. Zhou, Y. Zhang, Z.Y. Wang, W. Wei, W.F. Tang, J. Shi, R. Xiong, Appl. Surf. Sci. 254 (2008) 6972–6975.
[31] G.B. Ji, S.L. Tang, S.K. Ren, F.M. Zhang, B.X. Gu, Y.W. Du, J. Crystal Growth 270 (2004) 156–161.
[32] A. Lisfi, C.M. Williams, J. Appl. Phys. 93 (2003) 8143–8145.
[33] M. Rajendran, R.C. Pullar, A.K. Bhattacharya, D. Das, S.N. Chintalapudi, C.K. Majumdar, J. Magn. Magn. Mater. 232 (2001) 71–83.
[34] P.C.R. Varma, R.S. Manna, D. Banerjee, M.R. Varma, K.G. Suresh, A.K. Nigam, J. Alloys Compd. 453 (2008) 298–303.
[35] M.M. El-Okr, M.A. Salem, M.S. Salim, R.M. El-Okr, M. Ashoush, H.M. Talaat, J. Magn. Magn. Mater. 323 (2011) 920–926.
[36] P. Zaumseil, T. Schroeder, J. Phys. D: Appl. Phys. 44 (2011) 055403.